An increase in MECP2 dosage impairs neural tube formation

Paolo Petazzi[1#], Naiara Akizu[2#], Alejandra García[2], Conchi Estarás[2], Alexia Martinez de Paz[1], Manuel Rodriguez-Paredes[1], Marian A. Martínez-Balbás[2], Dori Huertas[1*] and Manel Esteller[1,3,4*]

[1]Cancer Epigenetics and Biology Program (PEBC), Bellvitge Biomedical Research Institute (IDIBELL), 08908 L'Hospitalet, Barcelona, Catalonia, Spain.

[2]Department of Molecular Genomics, Instituto de Biología Molecular de Barcelona, Consejo Superior de Investigaciones Científicas, Barcelona, Catalonia, Spain.

[3]Department of Physiological Sciences II, School of Medicine, University of Barcelona, Barcelona, Catalonia, Spain.

[4]Institucio Catalana de Recerca i Estudis Avançats (ICREA), Barcelona, Catalonia, Spain.

[#]Equally contributing authors

*Authors for correspondence (dhuertas@idibell.cat or mesteller@idibell.cat)

Abstract

Epigenetic mechanisms are fundamental for shaping the activity of the central nervous system (CNS). Methyl-CpG binding protein 2 (MECP2) acts as a bridge between methylated DNA and transcriptional effectors responsible for differentiation programs in neurons. The importance of MECP2 dosage in CNS is evident in Rett Syndrome and MECP2 duplication syndrome, which are neurodevelopmental diseases caused by loss-of-function mutations or duplication of the MECP2 gene, respectively. Although many studies have been performed on Rett syndrome models, little is known about the effects of an increase in MECP2 dosage. Herein, we demonstrate that MECP2 overexpression affects neural tube formation, leading to a decrease in neuroblast proliferation in the neural tube ventricular zone. Furthermore, an increase in MECP2 dose provokes premature differentiation of neural precursors accompanied by greater cell death, resulting in a loss of neuronal populations. Overall, our data indicate that correct MECP2 expression levels are required for proper nervous system development.

Introduction

During development, mitotically active precursors located in the neuroepithelium give rise to specialized neuronal and glial cells that define the adult nervous system. To maintain the brain's complexity, neurons originating from the neural tube undergo mitotic quiescence. Therefore, neuronal differentiation encompasses an elaborate developmental program in which neurogenic and antiproliferative signals work together to guarantee the differentiated state. This developmental step is mediated by genetic and epigenetic factors. Among the latter, chromatin remodelers (Clapier and Cairns, 2009), histone variants (Kamakaka and Biggins, 2005), histone post-translational modifications (Kouzarides, 2007) and DNA methylation (Miranda and Jones, 2007) are strongly involved in regulating the proliferation and differentiation of neural precursor cells. The importance of this regulation is highlighted by several neurological disorders caused by mutations in epigenetic genes, such as Rett syndrome (RTT), alpha thalassemia/mental retardation X-linked syndrome,

Rubinstein–Taybi syndrome and Coffin–Lowry syndrome (Urdinguio et al., 2009).

Among the epigenetic regulators of the brain, methyl-CpG-binding proteins are responsible for reading the methylation code of DNA and therefore, for regulating gene transcription (Klose and Bird, 2006). In fact, a mutation in the best-known protein of this family, MECP2 (methyl-CpG binding protein 2), is responsible for RTT (Amir et al., 1999). MECP2 is a basic nuclear protein that acts mainly as a transcriptional repressor, preferentially binding to methylated DNA sequences (Klose et al., 2005 and Lewis et al., 1992). Although MECP2 is widely expressed, MECP2 levels are highest in the brain, principally in mature postmigratory neurons (Jung et al., 2003). MECP2 protein levels are low during embryogenesis and increase progressively during the postnatal period of neuronal maturation (Balmer et al., 2003 and Cohen et al., 2003). In addition to its necessary role in mature neuronal and glial cells, MECP2 has been implicated in neuronal specification during early embryogenesis in several species (Coverdale et al., 2004 and Stancheva et al., 2003). Moreover, MECP2 has been shown to promote neuronal differentiation of neural stem cells while repressing astrocyte differentiation (Tsujimura et al., 2009).

The striking finding that MECP2 nucleotide mutations or duplications cause Rett syndrome or MECP2 duplication syndrome, respectively, suggests that careful regulation of this gene is necessary for correct brain development and function, as both overexpression and reduced expression are associated with neurodevelopmental disorders (Collins et al., 2004 and del Gaudio et al., 2006). Intriguingly, a loss of MECP2 function and an increase in MECP2 dosage lead to clinically similar neurological disorders (Van Esch et al., 2005). However, although many studies have been performed on MECP2 loss-of-function models, little is known about the biological consequences of MECP2 overexpression in either the adult or developing brain.

Using a well-known developmental model, the chick embryo neural tube, we sought to investigate the effects of human MECP2 overexpression on the proliferating progenitor

cells of neurons and glia. Here, we show that MECP2 dosage is fundamental for proper neural tube development and demonstrate that MECP2 overexpression provokes premature differentiation of proliferating progenitor cells. This ectopic differentiation leads to cell-cycle exit and cell death, ultimately resulting in decreased neuronal populations.

Materials and methods

Plasmids

The human MECP2_e1 full-length coding sequence was cloned into pCIG vector (Megason and McMahon, 2002). The vector comprises CMV enhancer and beta-actin promoter, followed by multiple cloning sites, internal ribosomal entry site (IRES) and a nuclear-localized green fluorescent protein (GFP).

Antibodies

The following primary antibodies were used: anti-MECP2 (Diagenode, custom); anti-BrdU (DSHB, G3G4); anti-phosphoH3S10 (Millipore, 05–806); anti-neural β-tubulin III (Tuj1) (R&D systems, MAB1195); anti HuC/D (Life Technologies, A-21271); anti-N-cadherin (R&D systems, AF6426); anti-active Caspase 3 (BD pharmingen, 559565); anti-active Caspase 8 (Millipore, MAB10754) and anti-β-actin-peroxidase (Sigma, A3854)

Chick in ovo electroporation

Eggs from White-Leghorn chickens were incubated at 38.5 °C and 70% humidity. Embryos were staged according to Hamburger and Hamilton (HH) (Hamburger and Hamilton, 1992). Chick embryos were electroporated with purified plasmid DNA at 2–3 μg/μl in H_2O with 50 ng/ml of Fast Green. Plasmid DNA was injected into the lumen of HH10 neural tubes, electrodes were placed at both sides of the neural tube and finally, the embryos were electroporated by an IntracelDual Pulse (TSS-100) delivering five 50 ms square pulses of 20–25 V.

mRNA extraction and RT-PCR

RNA was extracted with a Trizol reagent (Invitrogen) from dissected neural tubes according to the manufacturer's protocol. Single-stranded cDNA was synthesized with Thermoscript reverse-transcriptase and random hexamers (Life Technologies), and then subjected to PCR with the following primers: cMECP2, forward 5′-GGACCAGGAAGCTCAAACAGC-3′ and reverse 5′-TTGGGGCTCTTGGCTTTCTTG-3′; Gapdh, forward 5′-CTGAATGGGAAGCTTACTG-3′ and reverse, 5′-CATCATACTTGGCTGGTTTC-3′.

Western blotting

Neural tubes were dissected from several embryos at the same stage, pooled together and total protein was extracted with a Laemmli buffer. Equal amounts of protein (20 μg) were boiled for 10 min and β-mercaptoethanol was added to a 3% final concentration. Samples were then separated by electrophoresis on 10% SDS-PAGE gels, and transferred to nitrocellulose membranes. Membranes were blocked in 5% skim milk powder in PBS plus 0,1% Tween 20 for 1 h at room temperature and then incubated overnight at 4 °C with primary antibodies. For MECP2 (1:2000) antibody, an anti-rabbit HRP-conjugated secondary antibody (1:10,000) was used. Finally, complexes on the membrane were visualized using an ECL detection kit (GE Healthcare Life Sciences).

BrdU incorporation

Bromodeoxyuridine (BrdU, 0.5 μg/μl) was injected into the chick embryo neural tube lumen 30 min before fixation. Before anti-BrdU antibody incubation (which was performed as described below), the sections were treated with HCl 2 N for 30 min and washed with NaBorate 0.1 M (pH 8.5).

Indirect immunofluorescence

The collected brachial regions from embryos were fixed for 2 h at 4 °C in 4% paraformaldehyde, rinsed with PBS, soaked in a PBS 30% sucrose solution and embedded

in either OCT or agarose for sectioning in a Leica Cryostat (CM 1900) or a Vibratome (VT1000). The sections were blocked at room temperature for at least 1 h in 1% BSA (in PBS with 0.1% Triton X-100) before overnight incubation with primary antibodies at 4 °C. The sections were then incubated for 1.5 h at room temperature with Alexa-conjugated goat secondary IgG antibodies (Life Technologies) and 0.1 ng/µl DAPI (Sigma). Images were captured on a Leica SP5 confocal microscope using a 40 × oil-immersion objective and processed using a Fiji software. MECP2 intensity was quantified using the Fiji software as the following: each side of the neural tube (MECP2 EP and control) was selected as a region of interest (ROI) and the total intensity of all pixels for each ROI was calculated and compared.

Statistical analysis

Quantitative data were expressed as mean and standard error (s.e.). Significant differences between groups were tested by Student's *t*-test.

Results

Chicken MECP2 is expressed ubiquitously in the developing spinal cord

MECP2 is present in all vertebrates and is highly conserved among mammals, while divergence between mammalian and amphibian or fish MeCP2 more extensive. However, the alignment of chicken MECP2 with mouse and human MECP2 shows that the protein is highly conserved throughout species as diverse as humans and chickens. Although cMECP2 mRNA and protein are only partially annotated, a large part of the sequence is highly similar to human MECP2. Particularly striking is the 96.8% sequence identity in a 125-amino-acid region. Significantly, the conserved region includes the methyl-CpG binding domain (MBD) (Weitzel et al., 1997) (Fig. 1a). The high degree of conservation compares well with the characterization of the MBD as an essential element for binding of MECP2 to heterochromatin as well as unmethylated four-way DNA junctions (Galvão and Thomas, 2005 and Nan et al., 1996). Hence, we wondered whether cMECP2 (previously

known as *ARBP*) is expressed in the chicken embryo across different developmental stages. RT-PCR analysis of HH10, 20, 23 and 26 revealed that cMECP2 is indeed expressed in chick embryo (Fig. 1b) with greater expression seen at the HH20 stage. Since transcript presence does not always correlate with protein levels, we checked cMECP2 protein by western blot. Fig. 1c shows that cMECP2 is expressed at every tested developmental stage. Although in HH10 chick embryos the neural tube is formed mainly by the ventricular zone (VZ)—an epithelium composed entirely of mitotically active, multipotent neural precursor cells—from HH14 to 15 some of these neuroblasts exit the cell cycle and migrate laterally from the ventricular zone to the mantle zone (MZ), which is formed exclusively by post-mitotic, differentiating neurons and glia (Fig. 1d). Therefore, we wondered whether the MECP2 expression was restricted to the differentiating neurons or was global. To address this issue, we collected brachial sections of HH25 embryos and stained them with an anti-MECP2 antibody that recognizes the region shown in Fig. 1e. The chicken MECP2 partial annotated region shows high homology with the aminoacidic region of the mammalian MECP2 counterpart, thus, expecting that the antibody recognizes chicken MECP2 specifically (Weitzel et al., 1997). The results illustrate high expression of cMECP2 in ventral and in more dorsal ventricular cells as well as in mantle cells (Fig. 1f, top panel). Thus, MECP2 is present both in differentiated neurons and in neural progenitors. Moreover, we found that cMECP2 localizes in the nucleus, as staining of MECP2 overlaps with DAPI (Fig. 1f, bottom panel).

MECP2 overexpression reduces neuroblast proliferation

To investigate the role of a protein, lack and gain-of function studies are needed. The pCIG plasmid has been used in many gain-of-function studies to obtain new insights on genes function relevant for development, such as hJag1 (Neves et al., 2011), Wnt (Megason and McMahon, 2002), EZH2 (Akizu et al., 2010) and FGF (Martínez-Morales et al., 2011) among others, whose expression reached high levels when electroporated in ovo. Although different shRNA of the cMECP2 annotated region have been electroporated in chicken

embryo, none of them worked (data not shown).

Humans and mice have two protein isoforms produced by the alternative splicing of the MECP2/MECP2 gene with the MECP2E1 and E2 isoforms, differing only in their N-terminal sequences (Kriaucionis and Bird, 2004). It is known that MECP2E1-specific mutations alone are able to cause RTT (Gianakopoulos et al., 2012) and MECP2E1 displays 10 times more expression than E2 (Dragich et al., 2007). In addition, a recent study reported the differential distribution of MeCP2E1 within various brain regions in mice (Zachariah et al., 2012). With the aim to investigate the presence of different MECP2 isoforms in chicken we used a RT-PCR approach. Our exon-specific RT-PCR experiments based on the protein alignment between human and chicken and designed to amplify the sequence between Exons 1 and 3, failed to detect a second cMECP2 transcript (data not shown).

In order to analyze the effects of increased MECP2 dosage on the developing neural tube, we cloned MECP2_E1 full-length into a pCIG vector under the control of a CMV promoter. The additional expression of a nuclear-localized GFP from an internal ribosome entry site (IRES) enabled easy identification of transfected cells. In ovo injection of MECP2 expression plasmid into HH10 embryos and subsequent electroporation led to efficient and unilateral expression of this protein in the neural tube as it is shown in Fig. 2a, where the GFP channel colocalizes with the MECP2 red channel. Noteworthy, the pattern of nuclear localization of the endogenous protein is maintained upon MECP2 overexpression and the intensity of MECP2 signal is increased. Quantification of MECP2 intensity in electroporated (EP) neural tube compared with pCIG EP reveals an average of 45-fold more MECP2 in the electroporated region (Fig. 2a, graph). Although at 24 hours post-electroporation (PE) the neural tubes did not show any evidence of altered phenotypes, at 48 (data not shown) and 72 hours PE the thickness and the structure of electroporated neural tubes were highly affected, compared to the non-electroporated side or to the empty vector. The most striking feature associated with the overexpression of MECP2 was the

vastly reduced area occupied by the MZ, whose strong phenotype is appreciated in Figs. 2b, c, 3a, b and c.

To elucidate the mechanisms by which MECP2 overexpression so profoundly alters neural tube organization, we examined the proliferation rate of electroporated neural tubes. We took embryos at 72 h PE and processed them for bromodeoxyuridine (BrdU) staining, showing that MECP2 overexpression leads to an overall decrease in the number of proliferating BrdU positive cells (Fig. 2b). Noteworthy, the most affected part corresponds with higher levels of GFP (compare zoom squares of pCIG EP and MECP2 EP panels in Fig. 2b). In addition, in EP pCIG, GFP-labeled cells accumulated at the mantle zone due to the normal migration accompanying neuronal differentiation, while in EP MECP2 electroporated cells gathered mainly in the VZ, therefore making not possible to assess colocalization between GFP and BrdU. In order to quantify BrdU incorporation, BrdU labeled cells in control (pCIG) and MECP2 EP neural tubes were normalized with the total number of BrdU-positive cells in the respective non-EP side (graph of Fig. 2b). Results clearly indicate a reduction around 20% in BrdU levels as a result of MECP2 overexpression. We then wondered whether MECP2 overexpression affected also the levels of H3S10 phosphorylation, a histone mark that correlates with mitotically active cell populations. The H3S10p marker highlighted a mislocalization of actively dividing cells that normally reside close to the lumen. Again, higher levels of GFP coincide with disruption of H3S10p pattern (compare zoom square of pCIG EP and MECP2 EP panels in Fig. 2c). Quantification of anti-H3S10p immunostaining also showed that MECP2-electroporated neural tubes has a 20% decrease in the amount of mitotic cells than did the control neural tubes (Fig. 2c, graph). Collectively, these data emphasize the importance of proper spatial–temporal MECP2 expression for ensuring correct proliferation of progenitor cells residing in the ventricular zone of the neural tube.

MECP2 overexpression induces ectopic localization of differentiated neurons

Given that a role for MECP2 in promoting neuronal differentiation of neural precursor cells

has been proposed (Stancheva et al., 2003 and Tsujimura et al., 2009), we wondered whether the reduced proliferation of neural progenitor cells that we observed stemmed from premature induction of neurogenesis. To investigate this possibility, we took MECP2-electroporated neural tubes at 72 h PE, and then stained them with neural β-tubulin III (Tuj1), which is one of the earliest markers of neuronal commitment in primitive neuroepithelium. Fig. 3a show that MECP2 overexpression provokes a clear decrease in the amounts of differentiated neuronal population located at the mantle zone (compare zoom squares of pCIG control and MECP2 EP panels). Additionally, the same images of Tuj1 staining also show an ectopic localization of differentiated neurons in the MECP2-electroporated neural tubes. To confirm the phenotype caused by MECP2 overexpression, we immunostained with another marker, HuC/D, an RNA-binding protein specific to neuronal lineage. Again, when comparing MECP2 EP neural tubes with controls, depletion of differentiated cells is observed in MZ of MECP2 EP neural tubes (Fig. 3b, pCIG and MECP2 panels). This phenotype unequivocally shows an aberrant differentiation pattern for cells overexpressing MECP2, as it can be inferred by the presence of both GFP and Tuj1 in ectopically differentiated cells. Due to the non-nuclear localization of Tuj1 and HuC/D it has not been possible to quantify labeled cells of these markers. However, quantification of such qualitative markers was not necessary given that the difference in the level of staining of the mantle zone was striking, as well as it was the presence of Tuj1-stained cells in the VZ, which is normally populated by proliferating cells.

Since Tuj1 staining was found in the ventricular zone, we decided to check for neuroepithelial polarity markers, such as the cadherin family of proteins. In particular, the pattern of N-cadherin (Cdh2), a transmembrane protein that mediates homophilic adhesion at the cell junctions, was analyzed by immunostaining in the MECP2-electroporated neural tubes (at 72 h PE). The results clearly demonstrate that MECP2 overexpression disrupts the N-cadherin expression pattern along the lamina of the neural tube (Fig. 3c, compare zoom squares of control and MECP2 EP panels). This indicates that an increase in MECP2

dosage leads to a decrease in neuroepithelial polarity markers. These results suggest that, in addition to exiting the cell cycle and suffering from compromised polarity, MECP2-overexpressing neural precursor cells do not reach terminal differentiation, as can be inferred by reduced number of differentiating neurons in the MZ (Figs. 3a, c MECP2 panel).

MECP2 overexpression induces cell death

The observations that at 72 h PE the number of Tuj1 labeled cells in MECP2-electroporated neural tubes is vastly reduced, led us to analyze the rate of apoptosis before the onset of the altered phenotype. To this end, we determined the cellular levels of active Caspase-3 and – 8, two well-known serine proteases that are activated during the early-intermediate stages of apoptosis (reviewed in Parrish et al., 2013). Caspase-8 is classified as an initiator caspase and it is one of the earliest signals in the cascade, while Caspase-3 act downstream and can be cleaved, and therefore activated, by Caspase-8. Control pCIG EP neural tubes show very low levels of Caspase-3 and – 8 labeled cells as expected (Figs. 4a and b pCIG EP panel, graph 4c and 4d). However, the number of Caspase-3 and Caspase-8 labeled cells in MECP2 EP compared with pCIG EP neural tubes is significantly higher both at 24 and 48 h PE (Figs. 4a and b MECP2 EP panel, graph 4c and 4d). To confirm these data we quantified cells undergoing cell death by counting Dapi-positive nuclei showing the characteristic condensed morphology. Fig. 4e shows an increase of pyknotic cells in MECP2 EP, both at 24 and 48 h PE compared with pCIG EP neural tubes. These results clearly indicate the presence of apoptotic cells upon MECP2 electroporation and can explain the aberrant phenotype.

Discussion

To analyze the role of MECP2 in neurogenesis we have used a chicken model, however, we first checked whether our model was suitable for this purpose. First, expression of both cMECP2 transcript and protein has been detected in a wide window of developmental

stages. Then, we have found that chicken MECP2 is functionally analogous to its mammalian counterpart since its nuclear localization and the conservation of the region encompassing the methyl-CpG binding domain between human and chicken.

Our data also indicate that MECP2 overexpression causes neuroblasts to slow down proliferation, and that most of these neuroblasts die before they can reach terminal differentiation (Fig. 4f). Ectopic localization of differentiated neurons and reduced levels of polarity markers indicate that overexpression of MECP2 alone does not control the changes in polarity and migration that accompany neurogenesis. Neural cells die as a consequence of MECP2 overexpression, probably because they lack the additional spatial–temporal signals necessary for proper progression of neurogenesis. These results are in line with the lack of function studies from other models (Stancheva et al., 2003), indicating that the consequences of MECP2 overexpression do not represent toxic effects but specific ones.

Tsujimura et al. (2009) showed that MeCP2 overexpression in neural precursor cells (NPCs) promotes neuronal differentiation in adult mice. This work was based on the injection of embryo-derived NPCs in the brain or spinal cord of adult mice. We provided a more reliable study in which MECP2 ectopic expression has been induced in the chick neural tube without the need to deliver exogenous cells to the embryos. Our results are consistent with previous studies, which reported abnormally high levels of cell death in different in vitro systems overexpressing MECP2, relative to wild-type cells (Bracaglia et al., 2009 and Dastidar et al., 2012). Bracaglia et al. also reported that this pro-apoptotic effect disappears when the Rett syndrome-associated MECP2-R106W mutant, which is unable to bind to methylated DNA, is expressed—thereby implying that the MBD domain is essential for MECP2-induced apoptosis.

It is remarkable that *Xenopus laevis* MeCP2 was shown to regulate the number of neural precursor cells in the differentiating neuroectoderm of early *Xenopus* embryos (Stancheva et al., 2003). In the absence of MeCP2 protein, the expression of *Xenopus* Hairy2a (a member of the Hes family of proteins, which are regulated by the Notch/Delta signaling

pathway) was enhanced in embryos, which resulted in a lower number of differentiated neurons. Our results, together with the aforementioned study, highlight the importance of MECP2 dosage, as both knock-out and overexpression of this protein results in a reduced number of differentiated neurons. In our case, reduction in total number of cells is not due only to apoptosis but in addition there is a proliferation problem.

Interestingly, our phenotype resembles the one produced by the genetic ablation of Notch1 (de la Pompa et al., 1997). Loss of Notch signaling results in premature onset of neurogenesis by neuroepithelial cells of the midbrain–hindbrain region of the neural tube. Notch1-deficient cells do not complete differentiation but instead are eliminated by apoptosis, resulting in a reduced number of neurons in the adult cerebellum (Lütolf et al., 2002).

The molecular mechanism responsible of this phenotype can be explained by the relevant interactions between MECP2 and other proteins. For example, the MECP2-associated kinase HIPK2 has been shown to regulate cell growth and apoptosis, both in vivo and in vitro (Bracaglia et al., 2009). In addition, MECP2 interacts with many co-factors crucial for both proliferation and differentiation, such as HDAC2 (MacDonald et al., 2010) and NCOR/SMRT (Ebert et al., 2013).

This is the first study that investigates the consequences of MECP2 gain-of-function in the nervous system of an in-vivo model in the early stages of development. In particular, we introduce the novel idea that high expression of MECP2 in mitotic cells leads to anti-proliferative and apoptotic effects. Several cases of increased MECP2 copy number have been reported in male patients with progressive neurodevelopmental delay phenotype (Friez et al., 2006, Lugtenberg et al., 2006, Meins et al., 2005 and Van Esch et al., 2005). Interestingly, a male patient with triplication of the MECP2 locus was described to have an even worse early-onset neurological phenotype at 3 months of age (del Gaudio et al., 2006), suggesting that the severity of an MECP2 overexpression phenotype is proportional to the copy number increase. In order to reinforce this hypothesis, researchers have studied a

mouse model expressing seven times the wild-type levels of MeCP2 protein, reporting that it died by 3 weeks of age (Collins et al., 2004). Although the levels of MECP2 expression induced in the chicken neural tubes that we have described in the present study are not fully representative of the physiological situation in patients with MECP2-related disorders, our results are in line with lack and gain of function studies that elucidate the importance of correct gene dosage in neuronal development and disorders.

Conflict of interest

The authors declare that they have no conflict of interest.

Acknowledgments

This study was supported by the European Community's Seventh Framework Program (FP7/2007–2013), under grant agreement PITN-GA-2009-238242 and the project DISCHROM; ERC with grant agreement 268626; the project EPINORC; the E-RARE EuroRETT network (Carlos II Health Institute project PI071327); the Fondation Lejeune (France); MINECO projects SAF2011-22803, CSD2006-00049, BFU2009-11527 and BFU-2012-34261; Grant 090210 from Fundaciò La Marató de TV3; the Cellex Foundation; the Botín Foundation; the Catalan Association for Rett Syndrome; and the Health and Science Departments of the Catalan government (Generalitat de Catalunya). NA and CE received an I3P fellowship (I3P-BPD2005) and FPU fellowships respectively. ME is an ICREA Research Professor.

References

N. Akizu, C. Estarás, L. Guerrero, E. Martí, M.A. Martínez-Balbás
H3K27me3 regulates BMP activity in developing spinal cord
Development, 137 (2010), pp. 2915–2925

R.E. Amir, I.B. Van den Veyver, M. Wan, C.Q. Tran, U. Francke, H.Y. Zoghbi
Rett syndrome is caused by mutations in X-linked MECP2, encoding methyl-

CpG-binding protein 2
Nat. Genet., 23 (1999), pp. 185–188

D. Balmer, J. Goldstine, Y.M. Rao, J.M. LaSalle
Elevated methyl-CpG-binding protein 2 expression is acquired during postnatal human brain development and is correlated with alternative polyadenylation
J. Mol. Med., 81 (2003), pp. 61–68

G. Bracaglia, B. Conca, A. Bergo, L. Rusconi, Z. Zhou, M.E. Greenberg, N. Landsberger, S. Soddu, C. Kilstrup-Nielsen
Methyl-CpG-binding protein 2 is phosphorylated by homeodomain-interacting protein kinase 2 and contributes to apoptosis
EMBO Rep., 10 (2009), pp. 1327–1333

C.R. Clapier, B.R. Cairns
The biology of chromatin remodeling complexes
Annu. Rev. Biochem., 78 (2009), pp. 273–304

D.R. Cohen, V. Matarazzo, A.M. Palmer, Y. Tu, O.H. Jeon, J. Pevsner, G.V. Ronnett
Expression of MeCP2 in olfactory receptor neurons is developmentally regulated and occurs before synaptogenesis
Mol. Cell. Neurosci., 22 (2003), pp. 417–429

A.L. Collins, J.M. Levenson, A.P. Vilaythong, R. Richman, D.L. Armstrong, J.L. Noebels, J. David Sweatt, H.Y. Zoghbi
Mild overexpression of MeCP2 causes a progressive neurological disorder in mice
Hum. Mol. Genet., 13 (2004), pp. 2679–2689

L.E. Coverdale, C.J. Martyniuk, V.L. Trudeau, C.C. Martin
Differential expression of the methyl-cytosine binding protein 2 gene in embryonic and adult brain of zebrafish
Brain Res. Dev. Brain Res., 153 (2004), pp. 281–287

S.G. Dastidar, F.H. Bardai, C. Ma, V. Price, V. Rawat, P. Verma, V. Narayanan, S.R. D'Mello
Isoform-specific toxicity of MeCP2 in postmitotic neurons: suppression of neurotoxicity by FoxG1
J. Neurosci., 32 (2012), pp. 2846–2855

J.L. de la Pompa, A. Wakeham, K.M. Correia, E. Samper, S. Brown, R.J. Aguilera, T. Nakano, T. Honjo, T.W. Mak, J. Rossant, R.A. Conlon
Conservation of the Notch signalling pathway in mammalian neurogenesis
Development, 124 (1997), pp. 1139–1148

D. del Gaudio, *et al*.
Increased MECP2 gene copy number as the result of genomic duplication in neurodevelopmentally delayed males
Genet. Med., 8 (2006), pp. 784–792

J.M. Dragich, Y.H. Kim, A.P. Arnold, N.C. Schanen
Differential distribution of the MeCP2 splice variants in the postnatal mouse brain
J. Comp. Neurol., 501 (2007), pp. 526–542

D.H. Ebert, H.W. Gabel, N.D. Robinson, N.R. Kastan, L.S. Hu, S. Cohen, A.J. Navarro, M.J. Lyst, R. Ekiert, A.P. Bird, M.E. Greenberg
Activity-dependent phosphorylation of MeCP2 threonine 308 regulates interaction with NCoR
Nature, 499 (2013), pp. 341–345

M.J. Friez, J.R. Jones, K. Clarkson, H. Lubs, D. Abuelo, J.A. Bier, S. Pai, R. Simensen, C. Williams, P.F. Giampietro, C.E. Schwartz, R.E. Stevenson
Recurrent infections, hypotonia, and mental retardation caused by duplication of MECP2 and adjacent region in Xq28
Pediatrics, 118 (2006), pp. e1687–e1695

T.C. Galvão, J.O. Thomas
Structure-specific binding of MeCP2 to four-way junction DNA through its methyl CpG-binding domain
Nucleic Acids Res., 33 (2005), pp. 6603–6609

P.J. Gianakopoulos, Y. Zhang, N. Pencea, M. Orlic-Milacic, K. Mittal, C. Windpassinger, S.J. White, P.M. Kroisel, E.W. Chow, C.J. Saunders, *et al*.
Mutations in MECP2 exon 1 in classical Rett patients disrupt MECP2_e1 transcription, but not transcription of MECP2_e2
Am. J. Med. Genet. B Neuropsychiatr. Genet., 159B (2012), pp. 210–216

V. Hamburger, H.L. Hamilton
A series of normal stages in the development of the chick embryo. 1951
Dev. Dyn., 195 (1992), pp. 231–272

B.P. Jung, D.G. Jugloff, G. Zhang, R. Logan, S. Brown, J.H. Eubanks
The expression of methyl CpG binding factor MeCP2 correlates with cellular differentiation in the developing rat brain and in cultured cells
J. Neurobiol., 55 (2003), pp. 86–96

R.T. Kamakaka, S. Biggins
Histone variants: deviants?
Genes Dev., 19 (2005), pp. 295–310

R.J. Klose, A.P. Bird
Genomic DNA methylation: the mark and its mediators
Trends Biochem. Sci., 31 (2006), pp. 89–97

R.J. Klose, S.A. Sarraf, L. Schmiedeberg, S.M. McDermott, I. Stancheva, A.P. Bird
DNA binding selectivity of MeCP2 due to a requirement for A/T sequences adjacent to methyl-CpG
Mol. Cell, 19 (2005), pp. 667–678

T. Kouzarides
Chromatin modifications and their function
Cell, 128 (2007), pp. 693–705

S. Kriaucionis, A. Bird
The major form of MECP2 has a novel N-terminus generated by alternative splicing
Nucleic Acids Res., 32 (2004), pp. 1818–1823

J.D. Lewis, R.R. Meehan, W.J. Henzel, I. Maurer-Fogy, P. Jeppesen, F. Klein, A. Bird
Purification, sequence, and cellular localization of a novel chromosomal protein that binds to methylated DNA
Cell, 69 (1992), pp. 905–914

D. Lugtenberg, A.P. de Brouwer, T. Kleefstra, A.R. Oudakker, S.G. Frints, C.T. Schrander-Stumpel, J.P. Fryns, L.R. Jensen, J. Chelly, C. Moraine, G. Turner, J.A. Veltman, B.C. Hamel, B.B. de Vries, H. van Bokhoven, H.G. Yntema
Chromosomal copy number changes in patients with non-syndromic X linked mental retardation detected by array CGH
J. Med. Genet., 43 (2006), pp. 362–370

S. Lütolf, F. Radtke, M. Aguet, U. Suter, V. Taylor
Notch1 is required for neuronal and glial differentiation in the cerebellum
Development, 129 (2002), pp. 373–385

J.L. Macdonald, A. Verster, A. Berndt, A.J. Roskams
MBD2 and MeCP2 regulate distinct transitions in the stage-specific differentiation of olfactory receptor neurons
Mol. Cell. Neurosci., 44 (2010), pp. 55–67

P.L. Martínez-Morales, R. Diez del Corral, I. Olivera-Martínez, A.C. Quiroga, R.M. Das, J.A. Barbas, K.G. Storey, A.V. Morales
FGF and retinoic acid activity gradients control the timing of neural crest cell emigration in the trunk
J. Cell Biol., 194 (2011), pp. 489–503

S.G. Megason, A.P. McMahon
A mitogen gradient of dorsal midline Wnts organizes growth in the CNS
Development, 129 (2002), pp. 2087–2098

M. Meins, J. Lehmann, F. Gerresheim, J. Herchenbach, M. Hagedorn, K. Hameister, J.T. Epplen
Submicroscopic duplication in Xq28 causes increased expression of the MECP2 gene in a boy with severe mental retardation and features of Rett syndrome

J. Med. Genet., 42 (2005), p. e12

T.B. Miranda, P.A. Jones
DNA methylation: the nuts and bolts of repression
J. Cell. Physiol., 213 (2007), pp. 384–390

X. Nan, P. Tate, E. Li, A. Bird
DNA methylation specifies chromosomal localization of MECP2
Mol. Cell. Biol., 16 (1996), pp. 414–421

J. Neves, C. Parada, M. Chamizo, F. Giráldez
Jagged 1 regulates the restriction of Sox2 expression in the developing chicken inner ear: a mechanism for sensory organ specification
Development, 138 (2011), pp. 735–744

A.B.. Parrish, C.D. Freel, S. Kornbluth
Cellular mechanisms controlling caspase activation and function
Cold Spring Harb. Perspect. Biol., 5 (2013)

I. Stancheva, A.L. Collins, I.B. Van den Veyver, H. Zoghbi, R.R. Meehan
A mutant form of MECP2 protein associated with human Rett syndrome cannot be displaced from methylated DNA by notch in Xenopus embryos
Mol. Cell, 12 (2003), pp. 425–435

K. Tsujimura, M. Abematsu, J. Kohyama, M. Namihira, K. Nakashima
Neuronal differentiation of neural precursor cells is promoted by the methyl-CpG-binding protein MECP2
Exp. Neurol., 219 (2009), pp. 104–111

R.G. Urdinguio, J.V. Sanchez-Mut, M. Esteller
Epigenetic mechanisms in neurological diseases: genes, syndromes, and therapies
Lancet Neurol., 8 (2009), pp. 1056–1072

H. Van Esch, M. Bauters, J. Ignatius, M. Jansen, M. Raynaud, K. Hollanders, D. Lugtenberg, T. Bienvenu, L.R. Jensen, J. Gecz, C. Moraine, P. Marynen, J.P. Fryns, G. Froyen
Duplication of the MECP2 region is a frequent cause of severe mental

retardation and progressive neurological symptoms in males
Am. J. Hum. Genet., 77 (2005), pp. 442–453

J.M. Weitzel, H. Buhrmester, W.H. Strätling
Chicken MAR-binding protein ARBP is homologous to rat methyl-CpG-binding protein MECP2
Mol. Cell. Biol., 17 (1997), pp. 5656–5666

R.M. Zachariah, C.O. Olson, C. Ezeonwuka, M. Rastegar
Novel MeCP2 isoform-specific antibody reveals the endogenous MeCP2E1 expression in murine brain, primary neurons and astrocytes
PLoS One, 7 (2012), p. e49763

Figure Legends

Figure1

cMECP2 is ubiquitously expressed in the developing spinal cord. (a) Protein sequences of chicken (Accession no. CAA74577), human (NP_001104262) and mouse (NP_001075448) MECP2 were aligned. The region inside the black box shows that the human sequence and the chicken sequence share 96.8% identity. MBD (yellow) and TRD (red) domains are highlighted. (b) RT-PCR on HH10, 20, 23 and 26 neural tube RNA extracts. Minus reverse transcriptase samples (– RT) are shown on the right. (c) Immunoblot on HH10, 20, 23 and 26 neural tubes. (d) Scheme showing the neural tube organization at HH10 and 25. (e) The cMeCP2 fragment is partly conserved with the human peptide recognized by the antibody. (f) HH25 embryos were dissected and brachial sections were stained for MECP2 (red) and DAPI (blue).

Figure 2

Neuroblast proliferation is reduced upon MECP2 overexpression. HH10 embryos were electroporated with MECP2 or the empty vector in a bicistronic plasmid containing EGFP. All sections were taken from the brachial region. (a) MECP2 immunostaining (red) of embryos at 72 h PE. The graph shows MECP2 area intensity of MECP2 EP neural tubes relative to the empty vector (pCIG). Intensities were quantified by a Fiji software. Data shows mean of n = 3 sections (from 3 different embryos). Error bars indicate s.e. *$p < 0.05$.

(b) BrdU immunostaining (red) of 72 h PE embryos. The magnified red boxes show the most affected regions. The graph shows the number of BrdU positive cells found in MECP2 EP neural tubes relative to pCIG. Data show the mean of $n = 9$ sections (from three embryos). Error bars indicate s.e. ***$p < 0.001$. (c) H3S10p immunostaining (blue). The magnified red boxes show the most affected regions. The graph shows the number of H3S10p positive cells found in MECP2 EP neural tubes relative to pCIG. Data for pCIG show the mean of $n = 8$ sections (from three embryos), for MECP2 $n = 12$ sections (from two embryos). Error bars indicate s.e. **$p < 0.01$.

Figure 3

MECP2 overexpression provokes ectopic localization of differentiated neurons. a Tuj1 immunostaining (gray, upper panel) of embryos at 72 h PE. GFP is shown in the lower panel. For MECP2 EP, two embryos are shown. The magnified red box shows ectopically differentiating neurons. b HuC/D immunostaining (gray, upper panel). For MECP2 EP, two embryos are shown. c N-cadherin immunostaining (gray, upper panel). The magnified red box shows disruption of the N-cadherin pattern by MECP2.

Figure 4

MECP2 overexpression induces cell death. (a–b) HH10 embryos were electroporated with MECP2 or empty vector. Embryonic sections (at 24 and 48 h PE) from brachial region were immunostained for Caspase 8 (a) (gray, lower panel) and Caspase 3 (b) (gray, lower panel). The red boxes in the MECP2 EP highlight the Caspase-positive spots. c–d The graphs show the number of Caspase 8 (c) and Caspase 3 (d) positive cells in MECP2 EP neural tubes relative to pCIG EP at 24 and 48 h PE (pCIG 24 and 48 h n = 12 sections from 6 embryos; MECP2 24 h n = 21 from 10 embryos; MECP2 48 h n = 13 from 6 embryos). Error bars indicate s.e. *$p < 0.05$; **$p < 0.01$; ***$p < 0.001$. (e) Quantification of cells showing pyknotic features in neural tubes at 24 and 48 h PE (pCIG 24 and 48 h n = 12 sections from 6 embryos; MECP2 24 h n = 21 from 10 embryos; MECP2 48 h n = 13 from 6 embryos). Error bars indicate s.e. **$p < 0.01$; ***$p < 0.001$. (f) Model for MECP2 overexpression consequences in neural tube.

Figure 1

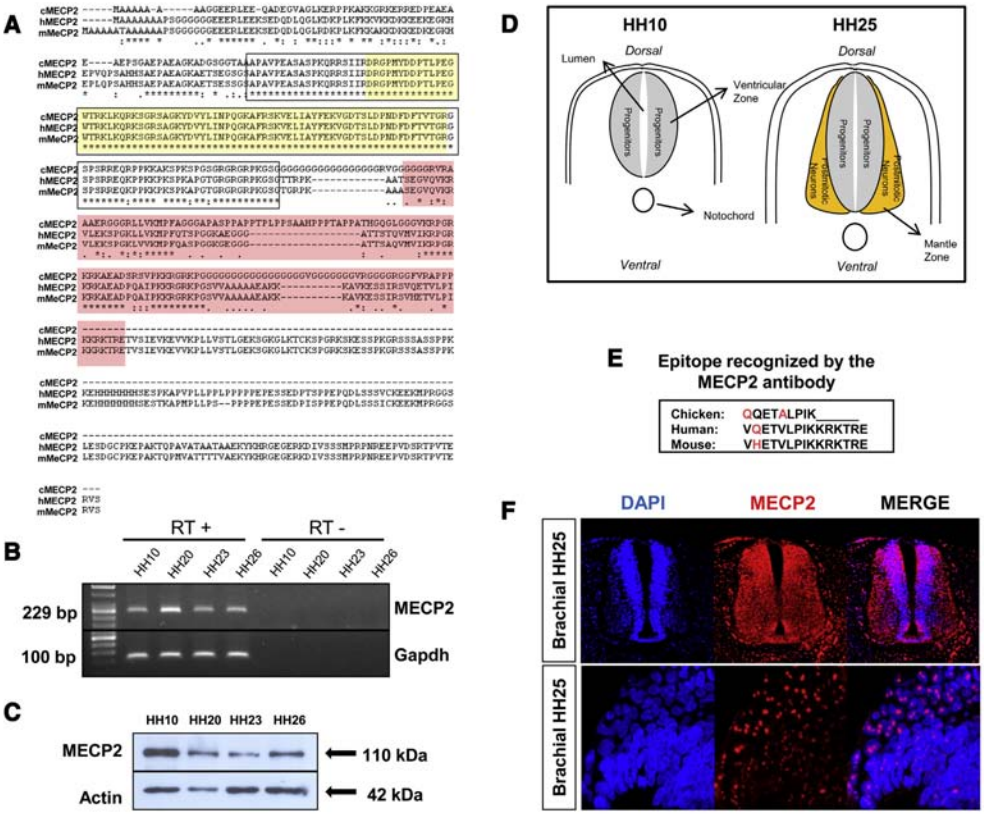
A
cMECP2
hMECP2
mMeCP2
B
RT +
RT -
HH10
HH20
HH23
HH26
229 bp
100 bp
MECP2
Gapdh
C
HH10 HH20 HH23 HH26
MECP2
Actin
110 kDa
42 kDa
D
HH10
HH25
Dorsal
Lumen
Ventricular Zone
Progenitors
Notochord
Ventral
Postmitotic Neurons
Mantle Zone
E
Epitope recognized by the MECP2 antibody
Chicken: QQETALPIK_____
Human: VQETVLPIKKRKTRE
Mouse: VHETVLPIKKRKTRE
F
DAPI
MECP2
MERGE
Brachial HH25
Brachial HH25

Figure 2

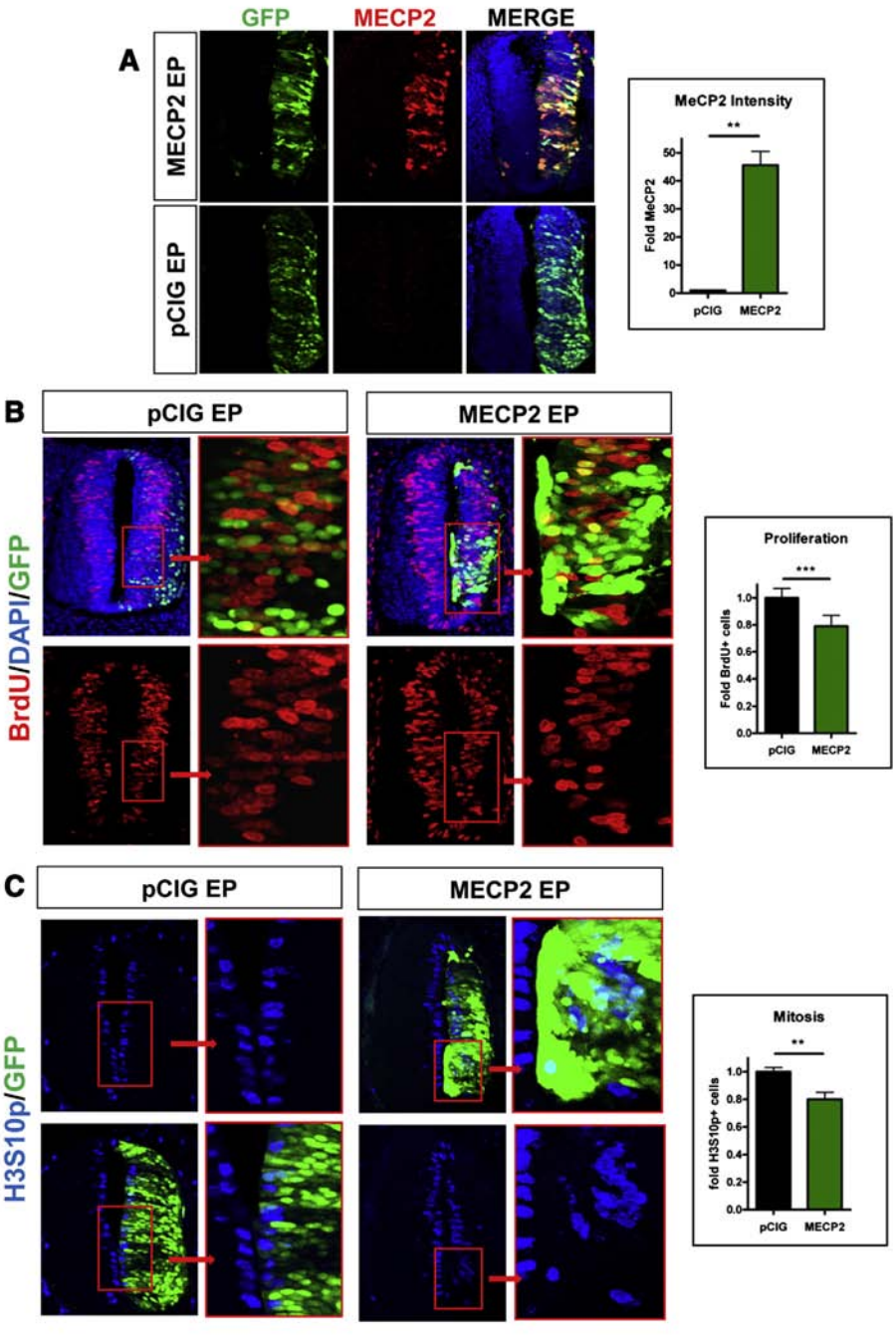
A
GFP
MECP2
MERGE
MECP2 EP
pCIG EP
MeCP2 Intensity
**
Fold MeCP2
pCIG
MECP2
B
pCIG EP
MECP2 EP
BrdU/DAPI/GFP
Proliferation
***
Fold BrdU+ cells
pCIG
MECP2
C
pCIG EP
MECP2 EP
H3S10p/GFP
Mitosis
**
fold H3S10p+ cells
pCIG
MECP2

Figure 3

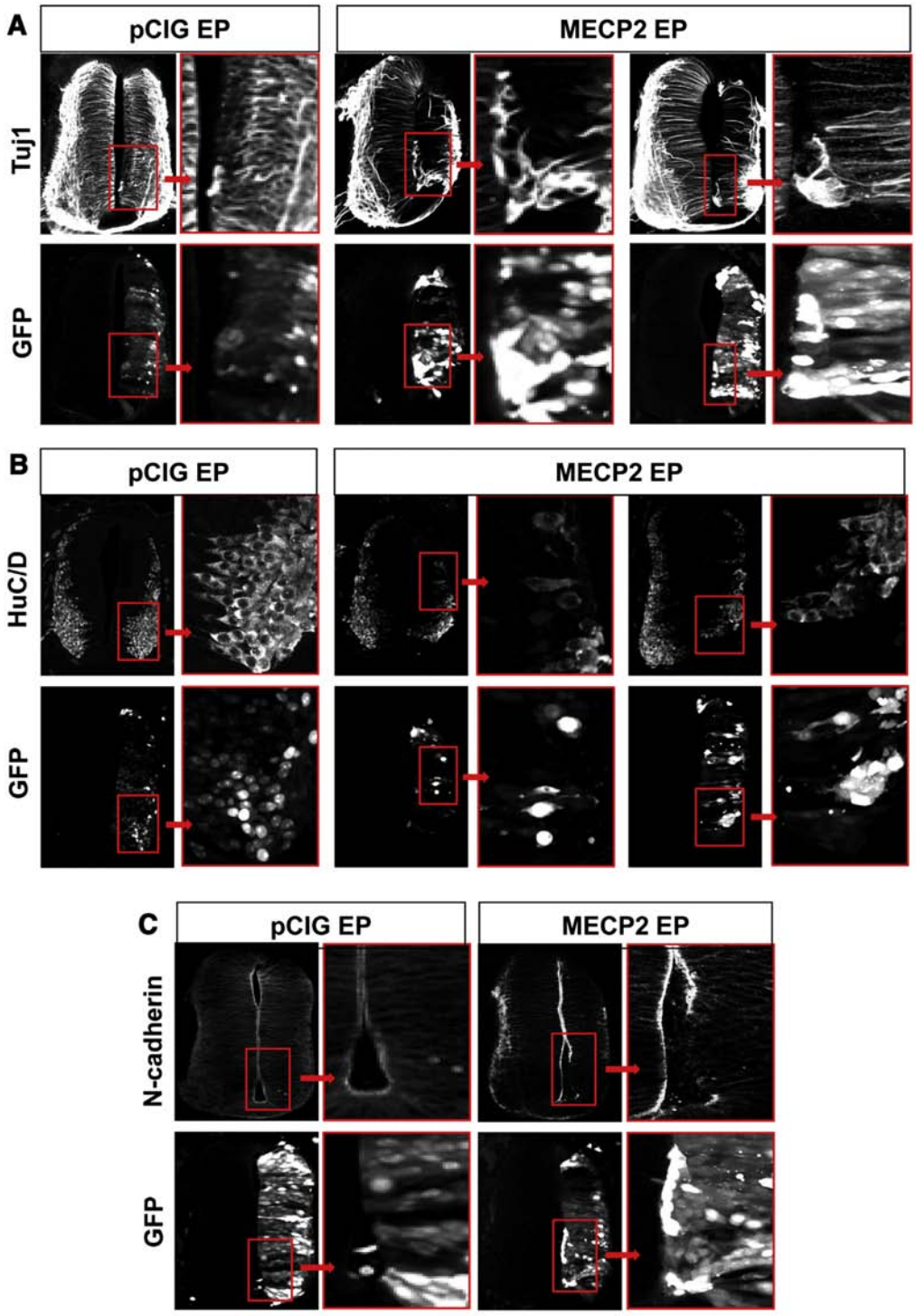
A
pCIG EP
MECP2 EP
Tuj1
GFP
B
pCIG EP
MECP2 EP
HuC/D
GFP
C
pCIG EP
MECP2 EP
N-cadherin
GFP

Figure 4

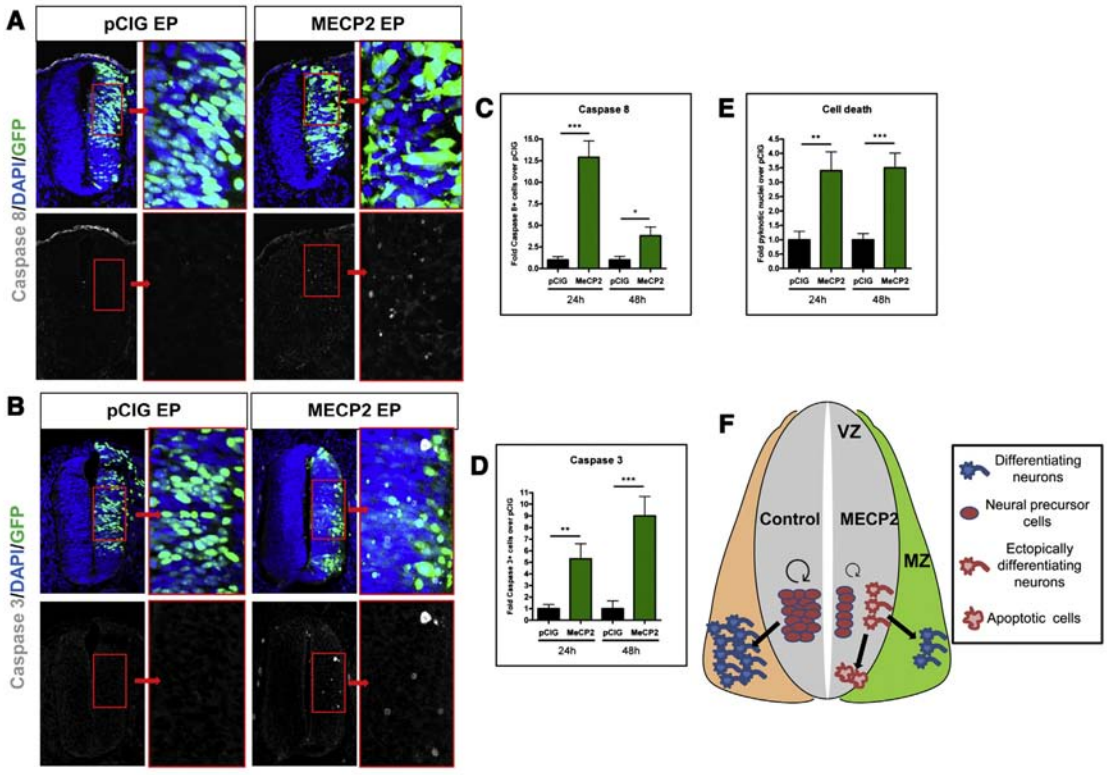
A
pCIG EP
MECP2 EP
Caspase 8/DAPI/GFP
B
pCIG EP
MECP2 EP
Caspase 3/DAPI/GFP
C
Caspase 8
pCIG
MeCP2
24h
48h
D
Caspase 3
E
Cell death
F
VZ
Control
MECP2
MZ
Differentiating neurons
Neural precursor cells
Ectopically differentiating neurons
Apoptotic cells